

## Energetic Localization of Saxitoxin in Its Channel Binding Site

Gaurav Choudhary,\* Lisa Shang,\* Xiufeng Li,\* and Samuel C. Dudley, Jr.\*†

\*Department of Medicine and †Department of Physiology, Emory University, Atlanta, Georgia 30322 USA and the Atlanta Veterans Administration Medical Center, Decatur, Georgia 30033 USA

**ABSTRACT** Saxitoxin (STX) selectively blocks the voltage-gated sodium channel at the outer vestibule lined by P-loops of the four domains. Neosaxitoxin has an additional -OH group at the N1 position of the 1,2,3 guanidinium (N1-OH) that interacts with domains I and IV of the Na<sup>+</sup> channel. Determination of a second toxin interaction with the channel would fix the location of STX. Gonyautoxin 2,3 and Gonyautoxin 1,4 are C-11 sulfated derivatives of saxitoxin and neosaxitoxin, respectively. We used these variants to constrain the STX docking orientation by energetically localizing the C-11 sulfate in the outer vestibule. Interactions between the C-11 sulfate and each of the four domains of the channel were determined by a systematic approach to mutant cycle analysis in which all known carboxyl groups important for site 1 toxin binding were neutralized, allowing energetic triangulation of the toxin sulfate and overcoming some limitations of mutant cycles. Toxin IC<sub>50</sub>s were measured by two-electrode voltage clamp from *Xenopus* oocytes injected with the channel mRNA. Three unique types of analysis based on the coupling results localized the C-11 sulfate between domains III and IV. Combined with our previous report, the data establish the orientation of STX in the outer vestibule and confirm the clockwise arrangement of the channel domains.

### INTRODUCTION

The voltage-gated Na<sup>+</sup> channel is critical for depolarization and conduction in most excitable cells. The channel is the target of many antiarrhythmic, anticonvulsant, and local anesthetic drugs. A basic property of the channel is its formation of a central pore by circumferential organization of four homologous domains, each with six transmembrane segments. The extracellular loops between the fifth and sixth transmembrane segments of each domain are called the pore-forming (P) loops. They fold back into the membrane to form the outer lining of the pore and the selectivity filter (Terlau et al., 1991; Favre et al., 1996; Sun et al., 1997).

Site 1 toxins block the channel by binding to the P-loops. Recently, we have proposed that the four domains are arranged in a clockwise configuration around the central axis of ion permeation site (Dudley et al., 2000; Li et al., 2001), based upon a pattern of P-loop interactions with site 1 toxin,  $\mu$ -conotoxin GIIIA. The asymmetrical marine neurotoxin, saxitoxin (STX), is a specific, high affinity ligand that binds in the same site (Fig. 1). Because of these properties, STX has played a critical role in the investigation of the Na<sup>+</sup> channel. The toxin has been useful in counting, localizing, purifying, and electrophysiologically studying the channel. Understanding toxin pharmacology is important because STX ingestion causes paralytic shellfish poisoning, a substantial public health threat. The mechanism by which this toxin binds the channel has been debated (Green and Andersen, 1986). Determining this could reveal inter-

esting biochemical characteristics of a high affinity site, and because of the rigid, known structure of the toxin, elucidation of toxin/channel interactions would set structural constraints on the outer vestibule. Recently, based upon the known shape of the toxin and experimentally determined interactions between the channel and a STX derivative, neosaxitoxin (neoSTX), we proposed a model explaining

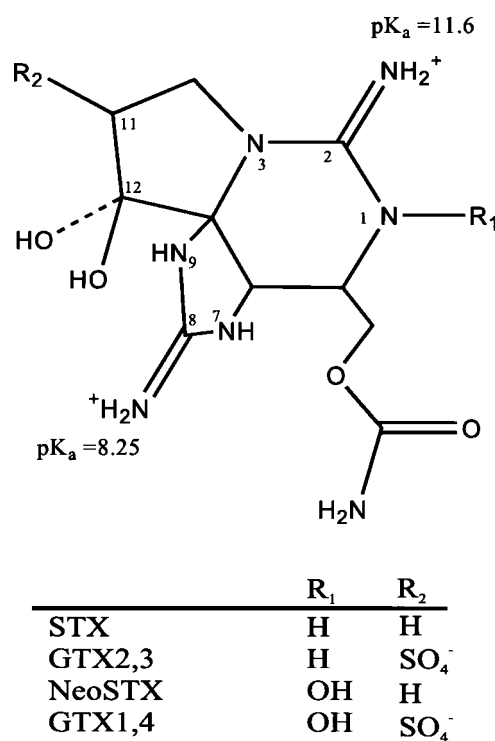


**FIGURE 1** Structure of STX and its analogs. NeoSTX and GTX1,4 have a hydroxyl group at N1 position, and the Gonyautoxins used have a sulfate group at C-11 position. The 7,8,9 guanidinium group is essential for toxin blocking.

Submitted November 22, 2001, and accepted for publication April 2, 2002.

Address reprint requests to Dr. Samuel C. Dudley, Jr., Assistant Professor of Medicine and Physiology, Division of Cardiology, Emory University/VAMC, 1670 Clairmont Road (111B), Decatur, GA 30033. Tel.: 404-329-4626; Fax: 404-329-2211; E-mail: sdudley@emory.edu.

© 2002 by the Biophysical Society

0006-3495/02/08/912/08 \$2.00

the known interactions and suggesting a mechanism of block (Penzotti et al., 2001). Independent determination of additional STX/channel interactions would help validate this model and have implications for channel architecture.

Gonyautoxins are another group of STX analogs that possess sulfate groups. Gonyautoxin 2,3 (GTX2,3) and Gonyautoxin 1,4 (GTX1,4) are epimeric mixtures of C-11 sulfated derivatives of saxitoxin and neosaxitoxin, respectively. In this study, we attempt to localize the sulfate by evaluating its interactions with all carboxyl groups from each of the four domains known to affect site 1 toxin binding. Interaction energies were determined by mutant cycle analysis. This approach, which we call energetic localization, should provide a relatively unbiased assessment of the orientation of C-11 sulfate with respect to the domain carboxyls and minimize any errors associated with mutant cycle analysis.

Mutant cycle analysis consists of comparing the interdependence of effects on affinity of mutations on the channel and on the toxin. The method allows for calculating the free energy of interaction between the two groups. The magnitude of this energy varies with the distance between the residues (Schreiber and Fersht, 1995). Because mutations of only carboxyls were used, implying a similar type of interaction, the interaction energy was used to estimate the spatial position of the C-11 sulfate with respect to each of the four channel domains.

## MATERIALS AND METHODS

### Preparation and expression of Na<sub>v</sub>1.4 channel

Most methods have been described previously in detail (Sunami et al., 1997; Penzotti et al., 2001). A brief description is provided. The Na<sub>v</sub>1.4 cDNA flanked by the *Xenopus* globulin 5' and 3' untranslated regions (provided by J. R. Moorman, University of Virginia, Charlottesville, VA) was subcloned into either the Bluescript SK vector or pAlter vector (Promega, Madison, WI). These vectors have been used extensively for oocytes expression of Na<sup>+</sup> channels. Oligonucleotide-directed point mutations were introduced into the adult rat skeletal muscle Na<sup>+</sup> channel (rNa<sub>v</sub>1.4 or SCN4a) by one of the following methods: mutation D400A by the Unique Site Elimination Mutagenesis Kit (Pharmacia Biotech, Piscataway, NJ), following the manufacturer's instructions; mutations E403Q, E758Q, D762N, E765Q, D1241A, and D1532N by four primer polymerase chain reaction (Higuchi, 1990). Oligonucleotides were designed with silent restriction site changes for rapid identification of mutants. DNA sequencing of the entire polymerized regions insured that only the intended mutations were present. The vectors were linearized and transcribed with a DNA-dependent RNA polymerase. Stage V and VI *Xenopus* oocytes from female frogs (NASCO, Ft. Atkinson, WI or Xenopus 1, Ann Arbor, MI) were injected with ~50 to 100 ng of cRNA. Oocytes were incubated at 16°C for 12 to 72 h prior to examination.

### Electrophysiology

Recordings were made in the two-electrode voltage clamp configuration using Dagan CA-1B oocyte clamp (Dagan Corp., Minneapolis, MN). Data were collected using Axograph 4.4 software (Axon Instruments, Foster City, CA). All recordings were obtained at room temperature (20–22°C).

The oocytes were placed in the center of a bath chamber designed to promote laminar flow, and the bath flow was typically 500  $\mu$ L/min. All determinations of blocking efficacy of STX, neoSTX, GTX2,3, and GTX1,4 for channel mutants were performed over the same time period and with oocytes injected simultaneously. The neoSTX affinity determinations for Na<sub>v</sub>1.4, D400A, and D1532N were previously reported by Penzotti et al. (2001). Affinity measurements for wild-type channels were reproducible over the experimental period.

A static bath was used to record D1532N affinity measurements because of high doses of Gonyautoxin required to calculate IC<sub>50</sub> (Stephan et al., 1994). The bath chamber was filled with 300  $\mu$ L of bath solution, and after achieving a baseline current, toxin was added to the solution to achieve a known final toxin concentration in the bath. The affinity measurements by this method were comparable with the flowing bath measurements for other channel mutants, validating the method.

The standard bath solution consisted of: 90 mM NaCl, 2.5 mM KCl, 1 mM CaCl<sub>2</sub>, 1 mM MgCl<sub>2</sub>, and 5 mM HEPES titrated to pH 7.2 with 1 N NaOH. STX was obtained from Sigma (St. Louis, MO), or the Marine Analytical Chemistry Standards Program of the Institute of Marine Biosciences, National Research Council of Canada (NRC, Halifax, Nova Scotia, Canada) and neoSTX, GTX2,3 (4.1:1 mixture of GTX2 and GTX3) and GTX1,4 (2.3:1 mixture of GTX1 and GTX4) from the NRC. STX from the various sources showed equivalent activity. Stocks were stored at –20°C and showed no degradation over the course of these experiments.

The effect of toxin addition was monitored by recording the peak current elicited every 20 s upon step pulses to 0 mV of 70-ms duration from a holding potential of –100 mV (Fig. 2). This protocol allowed the observation of toxin blocking and unblocking, insured equilibrium was reached, and avoided the development of use-dependent toxin block. There was no accumulation of inactivated channels with this stimulus rate for the wild-type or mutant channels studied. The IC<sub>50</sub> for toxin binding was calculated from the ratio of peak currents in the absence and presence of toxin based on a single site Langmuir adsorption isotherm.

### Mutant cycle analysis

We defined  $\Delta\Delta G$  as the difference of the  $\Delta G$  values for GTX1,4 and neoSTX, ( $\Delta\Delta G = (\Delta G_{\text{wild type, GTX}} - \Delta G_{\text{wild type, NeoSTX}}) - (\Delta G_{\text{mutant, GTX}} - \Delta G_{\text{mutant, NeoSTX}})$ ), where the first subscript position refers to the channel. The standard error of  $\Delta\Delta G$  was reported as the square root of the sum of the variances of the  $R7\ln$  (IC<sub>50</sub>) averages divided by the square root of the sum of the total number of observations minus four (Bevington, 1969). Note that  $\Delta\Delta G$  may be positive or negative, each representing a coupling interaction. The negative values represent less binding energy between the mutant pair as compared with the native residue pair. A positive  $\Delta\Delta G$  indicates that the introduced pair has more binding energy after mutation relative to the native pair. This may occur as a result of relief of repulsion or by addition of attraction.

Data are presented as means  $\pm$  SE. The number of observations ( $n$ ) was greater than or equal to 3 for all reported data. Statistical comparisons were performed using two-tailed Student's  $t$ -tests assuming unequal variances (Excel 2000, Microsoft Corp., Redmond, WA).

## RESULTS

The experimental design was to establish the affinity of the sulfated toxins for Na<sub>v</sub>1.4 and then to localize the C-11 sulfate within the channel's outer vestibule. Neutralization of all outer vestibule carboxyls known to affect site 1 toxins was undertaken to try to give a uniform and unbiased sampling of the energetic environment surrounding the C-11 sulfate group. All mutations introduced have been characterized, used in previously published work (Chahine

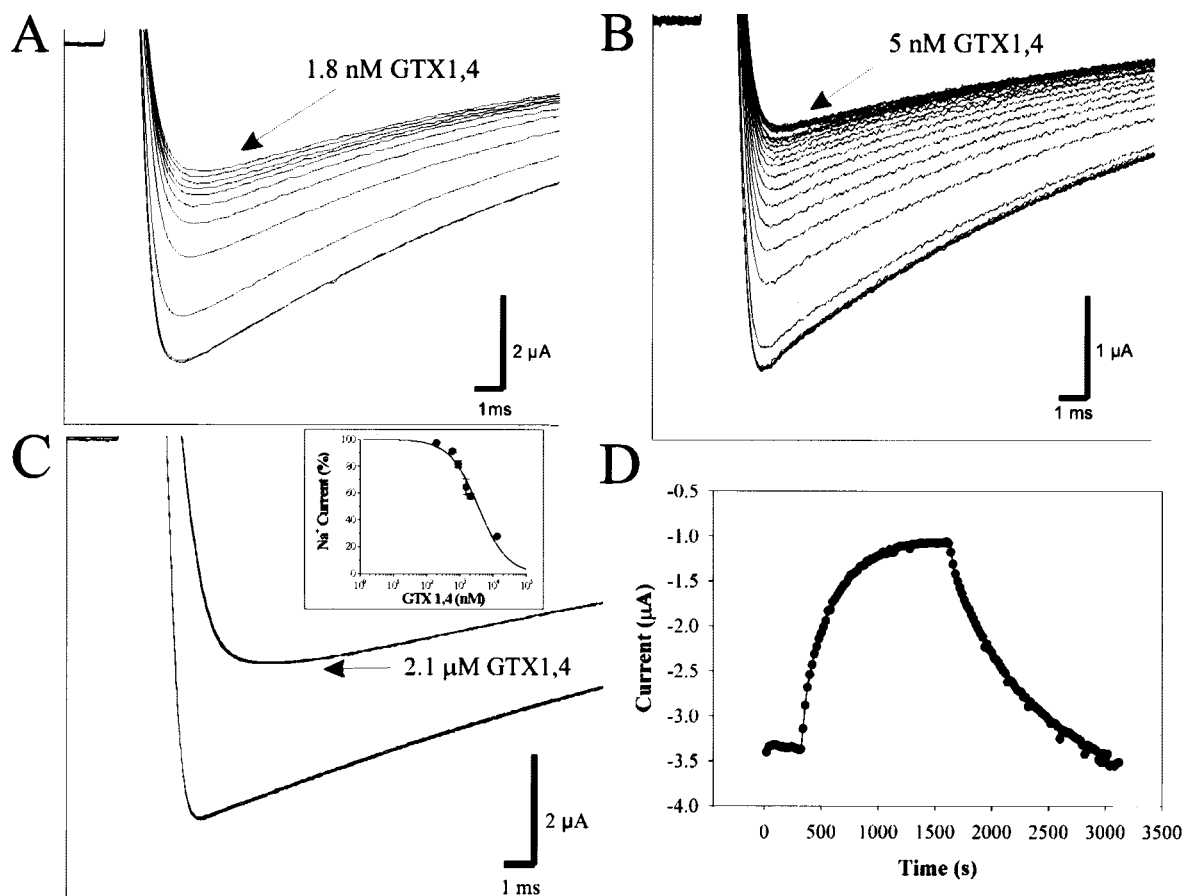


FIGURE 2 (A and B) Family of representative sodium current tracings using two-electrode voltage clamp from the  $\text{Na}_v1.4$  channel and mutation D1241A, respectively, expressed in *Xenopus* oocytes. Currents were elicited by depolarizing for  $70$  ms to  $0$  mV from a holding potential of  $-100$  mV every  $20$  s during the wash-in of toxin. Every third trace in the recording is shown. (C) Mutation D1532N in a static bath. Traces elicited using the same voltage step at baseline and after toxin addition are shown. (C Inset) Concentration-dependent inhibition of the  $\text{Na}^+$  current in oocytes injected with the D1532N mutant by GTX1,4 fitted to a single-site Langmuir isotherm ( $r^2 = 0.96$ ). (D) Peak current reduction and recovery measured from mutation D1241A upon addition of  $5$  nM GTX1,4. After equilibrium was reached with GTX1,4, the toxin was removed and the current came back to baseline.

et al., 1998; Li et al., 2001; Dudley et al., 1995, 2000; Sunami et al., 1997; Penzotti et al., 1998, 2001), and have been shown to have little effect on macroscopic gating parameters and  $\text{Na}^+$  selectivity.  $\text{IC}_{50}$  values were obtained from all the carboxyl residues in the outer ring of the vestibule except E403, because this mutation abolished binding completely (Terlau et al., 1991).

### Gonyautoxins block the wild-type channel

Gonyautoxins blocked the  $\text{rNa}_v1.4$  channels with the half blocking concentrations for GTX2,3 and GTX1,4 for  $\text{rNa}_v1.4$  of  $13.2 \pm 1.0$  nM and  $1.0 \pm 0.1$  nM, respectively (Fig. 3). Both sulfated toxins were approximately three-fold less potent than their nonsulfated counterparts, STX ( $4.1 \pm 0.1$  nM) and neoSTX ( $0.4 \pm 0.1$  nM). Also, GTX1,4 had 13-fold greater affinity compared with GTX2,3, a trend similar to that of neoSTX and STX for  $\text{Na}_v1.4$ . The presence of N1-OH conferred better binding with or without

C-11 sulfate. To further evaluate the affects of channel residue mutations on the binding, the neoSTX/GTX1,4 pair was chosen because these toxins had higher affinity.

### Channel mutations had variable effects on toxin binding

All carboxyl groups known to be involved with site 1 toxin binding were tested for their effect on neoSTX and GTX1,4 binding (Table 1). The mutations introduced have been used and characterized in the past by several authors (Chahine et al., 1998). Here and elsewhere, they showed no substantial change in macroscopic gating or  $E_{\text{rev}}$  (Li et al., 2001; Dudley et al., 1995, 2000; Sunami et al., 1997; Penzotti et al., 1998, 2001), implying no large structural changes. All mutations reduced affinity for neoSTX and GTX1,4 compared with the wild-type channel. The reduction in GTX1,4 affinity ranged from threefold for E765Q to 16,000-fold for E755A. Compared with  $\text{Na}_v1.4$ , mutations of domain I

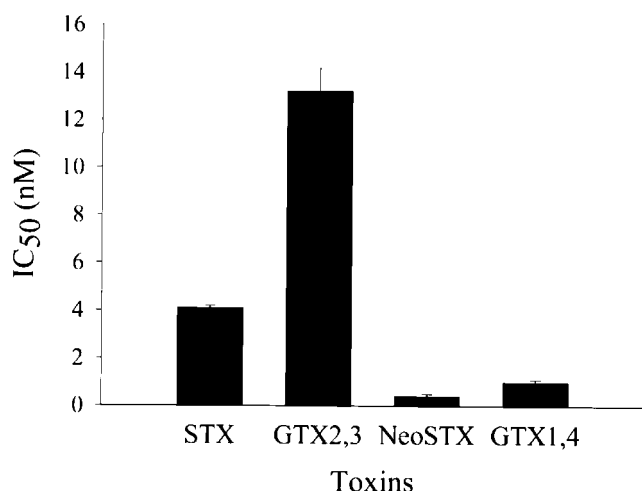


FIGURE 3 IC<sub>50</sub> values for the Na<sub>v</sub>1.4 channel of the sulfated toxins, GTX2,3 and GTX1,4, along with their nonsulfated counterparts, STX and neoSTX. Both GTX2,3 and GTX1,4 bind with less affinity compared with their nonsulfated counterparts STX and neoSTX, respectively. Data are presented as mean  $\pm$  SE.

residue D400A significantly decreased affinity of GTX1,4 by 30-fold ( $p < 0.05$ ), and domain I residue E403Q appeared to abolish binding completely. Domain II mutations D762N and E765Q had similar binding affinity for GTX1,4 ( $p =$  not significant), whereas domain II E755A and E758Q impaired binding affinity of GTX1,4 by 16,000-fold and 2400-fold, respectively. A statistically significant affinity decrease was noted with domain III mutation D1241A ( $p < 0.01$ ), and domain IV mutation D1532N led to a substantial decrease in binding with GTX1,4 ( $p < 0.01$ ). Even with the significantly reduced IC<sub>50</sub>, the concentration-dependent in-

hibition of the D1532N mutant by GTX1,4 was well described by a single-site Langmuir isotherm (Fig. 2 C). Allowing the Hill coefficient to vary resulted in a regression coefficient of 0.96 with a Hill coefficient of  $0.9 \pm 0.1$ . Although not excluding the possibility entirely, a Hill coefficient close to 1.0 suggested that any rearrangements of neoSTX in its binding site as the result of the relief of constraints associated with D1532/toxin interactions were likely to be minimal.

The trends for neoSTX were similar to those of GTX1,4, but there were quantitative differences. As expected for a positively charged toxin, no neutralization of a carboxyl group improved affinity. In decreasing order, residues D1532N, E755A, E758Q, D400A, D1241A, D762N, and E765Q were determinants of affinity. Compared with Na<sub>v</sub>1.4, reduced affinity for neoSTX resulted from mutations of domain II residues, E755A and E758Q ( $p < 0.01$ ), and of domain III residue D1241A ( $p < 0.01$ ). Domain II mutations, D762N and E765Q, caused no significant change in binding affinity for NeoSTX ( $p =$  NS), however. As previously reported, D400A ( $p < 0.01$ ) and D1532N ( $p < 0.01$ ) had lesser affinities compared with Na<sub>v</sub>1.4 (Penzotti et al., 2001).

### Gonyautoxin/channel interactions

The effect of single mutations on GTX1,4 and neoSTX binding suggested that domain I residue D400A, domain II residues E755A and E758Q, and domain IV residue D1532N were important for overall toxin binding, and all the channel mutations decreased binding with GTX1,4 compared with neoSTX except D1532N and D1241A. They improved GTX1,4 binding by 10-fold and 1.5-fold, respectively. To isolate the interactions of the C-11 sulfate with the mutated residues, we performed double mutant cycle analysis (Fig. 4).

Mutant cycle analysis showed a domain-specific pattern of interactions progressing from domains I to IV. The domain I residue had minimal interactions with the C-11 sulfate (D400,  $0.3 \pm 0.1$  kcal/mol). Moreover, the domain II residues E755, D762, and E765 had limited interaction with the C-11 sulfate (E755,  $0.3 \pm 0.2$  kcal/mol; D762,  $-0.0 \pm 0.2$  kcal/mol; and E765,  $-0.3 \pm 0.2$  kcal/mol). E758 of domain II had substantial interaction with the C-11 sulfate (E758,  $0.7 \pm 0.1$  kcal/mol). D1241A in domain III showed a strong coupling with the C-11 sulfate ( $\Delta\Delta G = 1.0 \pm 0.1$  kcal/mol), and domain IV residue D1532 showed the largest coupling ( $\Delta\Delta G = 2.0 \pm 0.1$  kcal/mol). Additionally, interactions were strongest with the more superficial carboxyls and progressively decreased with residues farther away from the ion permeation pathway (e.g., E765Q) or deeper into the pore (e.g., E755A) (Terlau et al., 1991). These results suggest that the C-11 sulfate group is located between domains III and IV at the superficial level in the outer vestibule.

TABLE 1 Changes in IC<sub>50</sub> of neoSTX and GTX1,4 with mutations of Na<sub>v</sub>1.4 channel

Residue	NeoSTX (nM)	GTX1,4 (nM)
Native channel	$0.3 \pm 0.1$ (9)	$1.0 \pm 0.1$ (7)
D400A	$16.3 \pm 1.1^*$ (8)	$30.9 \pm 4.5$ (3)
E403Q	ND	ND
E755A	$8200.0 \pm 990.9$ (4)	$16000.0 \pm 859.0$ (8)
E758Q	$2050.0 \pm 118.0$ (4)	$2430.0 \pm 49.3$ (8)
D762N	$1.8 \pm 0.1$ (3)	$6.5 \pm 1.5$ (3)
E765Q	$0.7 \pm 0.2$ (4)	$3.5 \pm 0.9$ (4)
D1241A	$2.1 \pm 0.1$ (4)	$3.3 \pm 0.1$ (3)
D1532N	$35600.0 \pm 2260.0^*$ (4)	$3580.0 \pm 468.0$ (20)

ND = Not determined.

\*Reported previously by Penzotti et al. (2001).



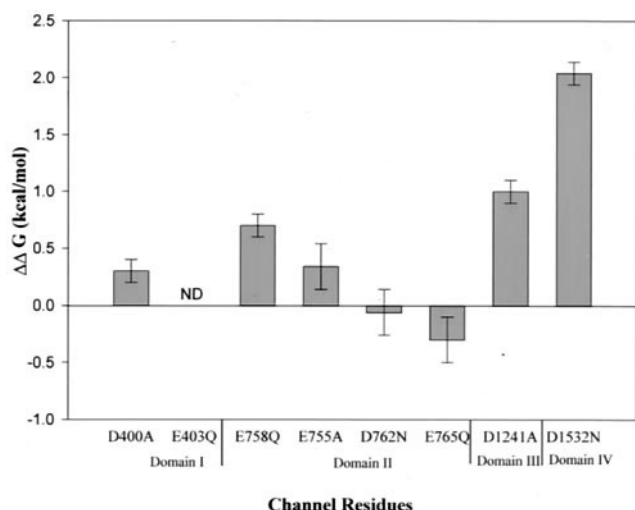


FIGURE 4 Interaction energies ( $\Delta\Delta G$ ) between various channel residues and the C-11 group of the toxin. Domain IV residue D1532 shows the largest interaction.

## Discussion

The purpose of the experiments was to energetically localize the C-11 group in relation to the domains of the outer vestibule of the sodium channel, further defining STX orientation within the outer vestibule and testing a previous proposal about toxin/channel interactions (Penzotti et al., 2001). The C-11 coupling with mutations of all outer vestibule carboxyls known to be important for site 1 toxin binding was evaluated. Carboxyl residues were chosen because of their important role in site 1 toxin binding. Moreover, carboxyl-sulfate interactions are likely to be of similar character making inferences of distance from energetic interactions more reliable. Carboxyls in all domains were evaluated to form a relatively unbiased sampling of those residues likely to contribute to the electrostatic field around C-11 group. Energetic localization has the additional benefit of minimizing any interpretive difficulties arising from any structural changes of channel mutants unaccounted by mutant cycles.

## Gonyautoxin block

In this study, the binding affinity of GTX2,3 and GTX1,4 with the  $\text{Na}_v1.4$  channel was determined for the first time, and as expected the toxins blocked current in a similar manner to previous experiments in other  $\text{Na}^+$  channels. In these studies, racemic mixtures of the toxins GTX2,3 and GTX1,4 were used. Previously, Kao and his colleagues reported the relative affinities of GTX2 and GTX3 compared with STX on giant squid axons (Kao et al., 1985). Assuming that they started with pure epimers, our results for  $\text{Na}_v1.4$  affinities are consistent with theirs after correcting for an epimeric mixture. There is a discrepancy between our

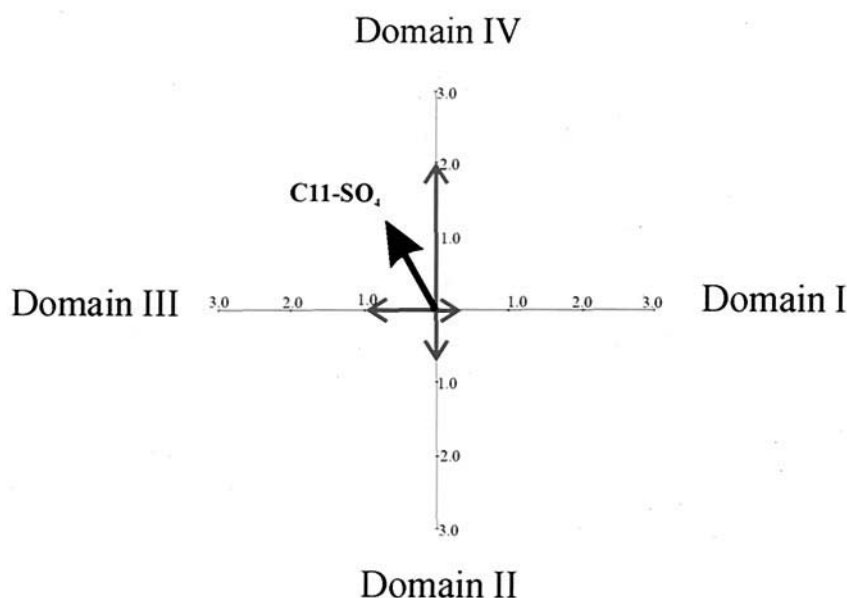
data and the relative potency for GTX1,4 as compared with neoSTX when calculated from data by Strichartz et al. (1986), however. In their data and using STX as a standard, the relative  $\text{IC}_{50}$  for neoSTX and GTX1,4 were 0.2 and 1.7 compared with our observations of 0.1 and 0.25, respectively. The GTX1,4 relative affinity difference may depend on the channel isoform, preparation, assay methods, and toxin purity. Any uncertainties introduced by the use of an epimeric mixture were not evaluated because of pure epimer availability and stability in solution.

The gonyautoxins bound less well to the  $\text{Na}_v1.4$  channel compared with their nonsulfated counterparts. This reduction in affinity is consistent with some repulsive interaction between the sulfate group and negatively charged amino acids forming the outer vestibule. Addition of a sulfate subtracts one positive charge from the toxin net charge and may alter the distribution of charge on the molecule. These changes might affect toxin binding or its voltage sensitivity. To explore the possibility of a change in partial charge distribution by addition of sulfate, we used computer simulation and partial charge calculations (Hyperchem, Hypercube, Inc., Gainesville, FL). Upon addition of the sulfate, the only change noted was in the N3 atom, where the partial charge changed less than 1%. This suggests that the sulfate group has only a minor effect on charge distribution of the 1,2,3 guanidinium group. Also, it seems unlikely that our measurements were affected significantly by a change in the voltage-dependence of binding. First, current was measured at 0 mV to help minimize any field effect. Second, the sulfate appears to bind superficially where the field drop should be small.

The effects of single mutations alone on toxin binding were insufficient to indicate important interactions between channel residues and the toxin C-11 sulfate. Mutations of domain I residue D400A, domain II residues E755A and E758Q, and domain IV residue D1532N had substantial effect on GTX1,4 binding. Nevertheless, when mutant cycle analysis was performed to isolate the interaction of the C-11 group with the channel residues, progressive coupling interactions of the C-11 sulfate with domain II E758Q, domain III D1241, and domain IV D1532 were identified. The reduced overall toxin binding observed with the mutations E755A and D400A were common to both neoSTX/GTX1,4, suggesting that although they are important for toxin binding, they do not interact with C-11. These results highlight the important role of mutant cycle analysis in evaluation of channel/ligand interactions.

Our results support coupling of the sulfate to several carboxyls, notably D1532, but the nature of these couplings is less clear. The sign of the  $\Delta\Delta G$ s was positive consistent with the removal of an unfavorable interaction between these carboxyls and the C-11 sulfate. The sulfate interactions are likely more complicated, however. For example, there was a 2.5-fold increase in the  $\text{IC}_{50}$  value for toxin binding with native channel by addition of C-11 sulfate. In

FIGURE 5 Based on the results of maximum likelihood analysis, the domains were arranged in a sequential clockwise manner and vector analysis of the interaction energies was performed. Significant interaction energies with each of the domains are plotted as vectors. On-axis arrows represent the  $\Delta\Delta G$  values for D400 in domain I, E758 in domain II, D1241 in domain III, and D1532 in domain IV. The off-axis vector represents the vector sum of energies pointing between domains III and IV.



the presence of D1532N, this effect changed to a 10-fold decrease in  $IC_{50}$ . Alternatively stated, the relative effect of mutating D1532 on binding of neoSTX (0.4–35600 nM) was greater than that on GTX1,4 binding (1.0–3580 nM). Although not eliminating the possibility of a D1532/sulfate repulsion, the improvement in binding to D1532N by adding the sulfate would be explained most easily by a new attractive force between Asn and the sulfate. This idea is consistent with the relative effects of introducing Asn in the 1532 site on neoSTX and GTX1,4. Nevertheless, the result would suggest that D1532 and the sulfate are near each other, and generation of new attractive forces is interpreted usually as suggesting specificity of the result (Chang et al., 1998).

### Energetic localization of C11 sulfate

We used mutant cycle analysis to energetically localize the C-11 group in the outer vestibule. The coupling data revealed that the maximum amount of interaction energy was with domain IV, localizing the C-11 group nearest this domain. Also, the interactions were maximal with the superficial carboxyl groups in the outer vestibule.

To confirm this interpretation based upon the highest energies of interaction, we analyzed the data by two independent methods, vector and likelihood analyses (Dudley et al., 2000). First, using the data of the N1-OH group's interactions from Penzotti et al. (2001) in addition to the data of C-11 sulfate interactions with all four domains, maximum likelihood analysis was performed. The only assumption made was that the domains were arranged in a circumferentially sequential manner. The sums of  $\Delta\Delta G$ s for each of the combinations of domain-toxin interactions were made and the variances calculated. The likelihood of a

particular orientation was taken as proportional to the sum of  $\Delta\Delta G$ s. The maximum likelihood was found to be with the C-11 sulfate pointing towards domain IV and the N1-OH pointing towards domain I when the domains were oriented in a clockwise manner as viewed from the extracellular surface. Second, all the significant interactions of the C-11 sulfate group were plotted as energy vectors pointing toward their respective domains, arranged in a clockwise circumferentially sequential manner as suggested by the likelihood analysis (Fig. 5). The resultant vector pointed in the direction between domain III and IV, closer to domain IV. Both of these analyses supported the intuitive conclusion of the C-11 sulfate location in the outer vestibule.

Although suggesting that the sulfate is closer to D1241, the interaction energies of the C-11 group are not significantly different for the E758 and D1241 mutations. Given the size of the vestibule, it seems possible that the sulfate could interact with multiple residues. Experimental variability in  $IC_{50}$  determination, inhomogeneity of the dielectric, and variable relative depth of the P-loops (Chiamvimonvat et al., 1996) might account for the lack of statistical difference. The subsequent analyses integrate the total data set, and all analyses support the conclusion that the sulfate is closest to domain IV. The lack of coupling between D762 and E765 is consistent with previous experiments, suggesting that these residues lie further away from and, in the case of E765, deeper in the permeation path (Li et al., 2000).

The sum of interaction energies between the C-11 sulfate and D1241 and D1532 is more than the change in binding energy from neoSTX to GTX1,4 with the native channel. This discrepancy is most likely the result of interactions not identified between the C-11 group and the channel and should not affect significantly our conclusions about the location of the C-11 group.

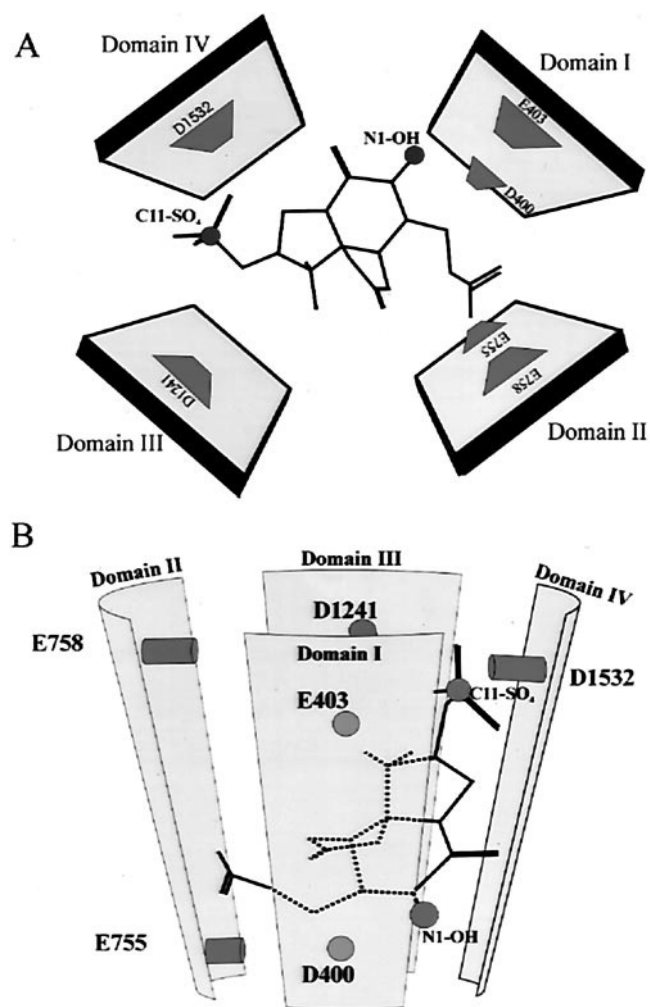


FIGURE 6 Schematic diagram showing the docking of GTX1,4 in the outer vestibule of Na<sub>v</sub>1.4, explaining data showing C-11 sulfate and N1-OH coupling. Based on recent data by Dudley et al. (2000) and Li et al. (2001) and the maximum likelihood analysis, the domains are arranged in a clockwise manner when viewed from outside. Selective residues important for STX binding are arranged along the axis of ion-permeation in accordance with electrical depth (Yamagishi et al., 1997). (A) Top view of the outer vestibule with GTX1,4 shown in stick figure; (B) Side view. Note that the C-11 sulfate approximates domains III and IV, and the N1-OH, domain I.

### Structural implications for the outer vestibule

These results allow determination of the binding orientation of STX with respect to the channel. We showed that the C-11 group on the toxin was located closest to domain IV (Fig. 6). Penzotti et al. (2000) showed that the N1-OH group lay closest to domain I residues near the selectivity filter (Penzotti et al., 2001). Previously published studies revealed that the 7,8,9 guanidinium group points towards the selectivity filter (Penzotti et al., 1998). These three interactions fix the orientation of STX with respect to the channel pore and support our previous docking proposal (Penzotti et al., 2001).

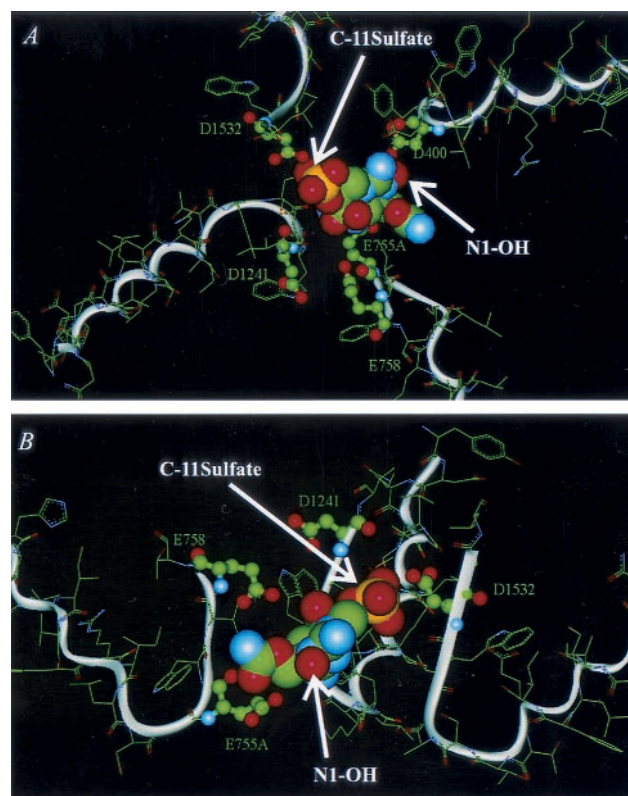


FIGURE 7 GTX1,4 docked in a molecular model of the outer vestibule as proposed by Lipkind and Fozzard (2000). This model accommodates GTX1,4 well, and the C-11 sulfate is located superficially between domain III and domain IV, compatible with the coupling data. Main features of the model include P-loops consisting of N-terminal helices, extended structures of the C-terminal pore lining segments and a clockwise arrangement of the domains as viewed from outside (Dudley et al., 2000; Li et al., 2001). GTX1,4 is shown in (Corey, Pauling and Kuntz) (CPK) format. Ribbons demonstrate the channel backbone. Channel amino acids previously shown to interact with N1-OH (Penzotti et al., 2001) or tested here are shown in ball and stick format. Domain II residues D762N and E765Q lie outside the modeled region of the pore and are not shown. Carbon is shown as green, oxygen red, nitrogen blue, sulfur yellow, and hydrogen white. (A) Top view from outside of the outer vestibule with GTX1,4 showing the domain III and domain IV interaction of the C-11 sulfate; (B) side view of the outer vestibule. The domain I P-loop has been removed for clarity.

This docking orientation has implications for the channel outer vestibule structure. First, the docking model is consistent with distance measurements made by Bénitah et al. (1996). They reported the distance between domain IV and domain I to be  $<10$  Å using paired cysteine mutagenesis studies and evaluating the likelihood of disulfide bond formation between paired residues (Bénitah et al., 1996). The measured distance between the oxygen atom at N1-OH and sulfur at C-11 group of GTX1,4 is  $\sim 7$  to 8 Å, consistent with the domain separation predicted. Second, the orientation of STX with respect to the domains provides an independent line of evidence using a second toxin in support of the clockwise arrangement of the domains as viewed from



the outer surface. Recently, by determining points of interaction between the channel and  $\mu$ -conotoxin GIIIA using mutant cycle analysis, Dudley et al. (2000) and Li et al. (2001) proposed that the four domains forming the outer vestibule are arranged in a clockwise manner (Dudley et al., 2000; Li et al., 2001). For the C-11 sulfate to be located near domain IV, N1-OH to be directed toward domain I, and the 7,8,9 guanidinium group to be oriented towards the selectivity filter the domains must be arranged in a clockwise manner. This conclusion was supported by our likelihood analysis of all clockwise and counter-clockwise sequential domain arrangements.

In this study, we show that the Gonyautoxins block the  $\text{Na}_v1.4$ , and we localize the C-11 group in the outer vestibule. These results establish the orientation of STX with respect to the channel and set constraints on the structure of the outer vestibule, an area of the channel involved in gating, selectivity, and drug recognition. The results are consistent with a previous model of STX docking and with the putative clockwise arrangement of the domains (Fig. 7). Future studies with other toxin analogs will improve our understanding of toxin/channel interactions and likely further constrain the outer vestibule model.

We thank Dr. Gregory Lipkind and Dr. Harry Fozzard for providing us the outer vestibule model and for constructive comments on the discussion. Also, we thank Dr. Jennifer L. Penzotti for sharing some of the affinity measurements for the native channel. Dr. Dudley is supported by a Scientist Development Award from the national American Heart Association, a Grant-In-Aid from Southeast Affiliate of American Heart Association, a Procter and Gamble University Research Exploratory Award, and a National Institutes of Health Award (HL64828).

## REFERENCES

- Bénitah, J. P., G. F. Tomaselli, and E. Marban. 1996. Adjacent pore-lining residues within sodium channels identified by paired cysteine mutagenesis. *Proc. Natl. Acad. Sci. U. S. A.* 93:7392–7396.
- Bevington, P. R. 1969. Propagation of errors. In *Data Reduction and Error Analysis for the Physical Sciences*. McGraw-Hill Book Company, New York. 56–65.
- Chahine, M., J. Sirois, P. Marcotte, L. Chen, and R. G. Kallen. 1998. Extrapore residues of the S5–S6 loop of domain 2 of the voltage-gated skeletal muscle sodium channel (rSkM1) contribute to the  $\mu$ -conotoxin GIIIA binding site. *Biophys. J.* 75:236–246.
- Chang, N. S., R. J. French, G. M. Lipkind, H. A. Fozzard, and S. Dudley, Jr. 1998. Predominant interactions between  $\mu$ -conotoxin Arg-13 and the skeletal muscle  $\text{Na}^+$  channel localized by mutant cycle analysis. *Biochemistry*. 37:4407–4419.
- Chiamvimonvat, N., M. T. Pérez-García, R. Ranjan, E. Marban, and G. F. Tomaselli. 1996. Depth asymmetries of the pore-lining segments of the  $\text{Na}^+$  channel revealed by cysteine mutagenesis. *Neuron*. 16:1037–1047.
- Dudley, S. C., N. Chang, J. Hall, G. Lipkind, H. A. Fozzard, and R. J. French. 2000.  $\mu$ -Conotoxin GIIIA interactions with the voltage-gated  $\text{Na}^+$  channel predict a clockwise arrangement of the domains. *J. Gen. Physiol.* 116:679–690.
- Dudley, S. C., Jr., H. Todt, G. Lipkind, and H. A. Fozzard. 1995. A  $\mu$ -conotoxin-insensitive  $\text{Na}^+$  channel mutant: possible localization of a binding site at the outer vestibule. *Biophys. J.* 69:1657–1665.
- Favre, I., E. Moczydlowski, and L. Schild. 1996. On the structural basis for ionic selectivity among  $\text{Na}^+$ ,  $\text{K}^+$ , and  $\text{Ca}^{2+}$  in the voltage-gated sodium channel. *Biophys. J.* 71:3110–3125.
- Green, W. N., and O. S. Andersen. 1986. Surface charges near the guanidinium neurotoxin binding site. *Ann. N. Y. Acad. Sci.* 479:306–312.
- Higuchi, R. 1990. Recombinant PCR. In *PCR Protocols: A guide to Methods and Applications*. M. A. Innis, editor. Academic Press, New York. 177–183.
- Kao, C. Y., P. N., Kao, M. R. James-Kracke, F. E. Koehn, C. F. Wichmann, and H. K. Schnoes. 1985. Actions of epimers of 12-(OH)-reduced saxitoxin and of 11-(OSO<sub>3</sub>)-saxitoxin on squid axon. *Toxicon*. 23:647–655.
- Li, R. A., I. I. Ennis, R. J. French, S. C. Dudley, Jr., G. F. Tomaselli, and E. Marban. 2001. Clockwise domain arrangement of the sodium channel revealed by  $\mu$ -conotoxin GIIIA docking orientation. *J. Biol. Chem.* 276:11072–11077.
- Li, R. A., P. Velez, N. Chiamvimonvat, G. F. Tomaselli, and E. Marban. 2000. Charged residues between the selectivity filter and S6 segments contribute to the permeation phenotype of the sodium channel. *J. Gen. Physiol.* 115:81–92.
- Lipkind, G. M., and H. A. Fozzard. 2000. KcsA crystal structure as framework for a molecular model of the  $\text{Na}^+$  channel pore. *Biochemistry*. 39:8161–8170.
- Penzotti, J. L., H. A. Fozzard, G. M. Lipkind, and S. C. Dudley, Jr. 1998. Differences in saxitoxin and tetrodotoxin binding revealed by mutagenesis of the  $\text{Na}^+$  channel outer vestibule. *Biophys. J.* 75:2647–2657.
- Penzotti, J. L., G. Lipkind, H. A. Fozzard, and S. C. Dudley. 2001. Specific neosaxitoxin interactions with the  $\text{Na}^+$  channel outer vestibule determined by mutant cycle analysis. *Biophys. J.* 80:698–706.
- Schreiber, G., and A. R. Fersht. 1995. Energetics of protein-protein interactions: analysis of the barnase-barstar interface by single mutations and double mutant cycles. *J. Mol. Biol.* 248:478–486.
- Stephan, M. M., J. F. Potts, and W. S. Agnew. 1994. The  $\mu$ I skeletal muscle sodium channel: mutation E403Q eliminates sensitivity to tetrodotoxin but not to  $\mu$ -conotoxins GIIIA and GIIIB. *J. Membr. Biol.* 137:1–8.
- Strichartz, G., T. Rando, S. Hall, J. Gitschier, L. Hall, B. Magnani, and C. H. Bay. 1986. On the mechanism by which saxitoxin binds to and blocks sodium channels. *Ann. N. Y. Acad. Sci.* 479:96–112.
- Sun, Y. M., I. Favre, L. Schild, and E. Moczydlowski. 1997. On the structural basis for size-selective permeation of organic cations through the voltage-gated sodium channel: effect of alanine mutations at the DEKA locus on selectivity, inhibition by  $\text{Ca}^{2+}$  and  $\text{H}^+$ , and molecular sieving. *J. Gen. Physiol.* 110:693–715.
- Sunami, A., S. C. Dudley, Jr., and H. A. Fozzard. 1997. Sodium channel selectivity filter regulates antiarrhythmic drug binding. *Proc. Natl. Acad. Sci. U. S. A.* 94:14126–14131.
- Terlau, H., S. H. Heinemann, W. Stuhmer, M. Pusch, F. Conti, K. Imoto, and S. Numa. 1991. Mapping the site of block by tetrodotoxin and saxitoxin of sodium channel II. *FEBS Lett.* 293:93–96.
- Yamagishi, T., M. Janacki, E. Marban, and G. F. Tomaselli. 1997. Topology of the P segments in the sodium channel pore revealed by cysteine mutagenesis. *Biophys. J.* 73:195–204.